Fractionally-Spaced Equalization:
An Improved Digital Transversal Equalizer

By R. D. GITLIN and S. B. WEINSTEIN

Here we describe and demonstrate, via analysis and simulation, the performance improvement of voice-grade modems which use a Fractionally-Spaced Equalizer (FSE) instead of a conventional synchronous equalizer. The reason for this superior performance is that the FSE adaptively realizes the optimum linear receiver; consequently it can effectively compensate for more severe delay distortion than the conventional adaptive equalizer, which suffers from aliasing effects. An additional advantage of the FSE is that data transmission can begin with an arbitrary sampling phase, since the equalizer synthesizes the correct delay during adaptation. We show that an FSE combined with a decision feedback section, which can mitigate the effect of severe amplitude distortion, can compensate for a wide range of linear distortion. At 9.6 kbit/s, the FSE provides a 2 to 3 dB gain in output signal-to-noise ratio, relative to the synchronous equalizer, over worst-case private-line channels. This translates to a theoretical improvement of approximately two orders of magnitude in bit error rate.

I. INTRODUCTION

As is well known,[1,2] high-speed ($\geq$4.8 kbit/s) voiceband modems must employ some sort of adaptive equalization to achieve reliable performance in the presence of linear distortion and additive noise. The equalizers are invariably implemented using transversal filters, but the question of how the taps should be spaced has been, and still is, of great theoretical as well as practical interest. Conventionally, the equalizer taps are spaced at the reciprocal of the signaling rate. While it has been known theoretically that this synchronous structure does not, by itself, realize the optimum linear filter, it has up to this time provided adequate performance. The continuing demand for improved

performance at 9.6 kbit/s has renewed interest in adaptive equalizers whose taps are spaced closer than the reciprocal of twice the highest frequency component in the baseband signal.[3-7] As we shall demonstrate, such Fractionally-Spaced Equalizers (FSEs) are able to compensate much more effectively for delay distortion than the conventional synchronous equalizers. Consequently, we will show that the performance of a FSE, with a sufficient number of taps, is almost independent of the channel delay distortion, and thus of the receiver sampling phase. More generally, the FSE is able to adaptively realize, in one device, the optimum linear receiver, which is known to be the cascade of a matched filter and a synchronously-spaced equalizer.[8]

The purpose of this paper is to report the results of an in-depth comparative analytical and simulation study of FSEs and the conventional synchronous equalizer. We also evaluate the performance of an equalizer which results when a decision-feedback section, which is particularly effective in compensating for amplitude distortion, is combined with an FSE. We present simulation results that compare the performance of practical-length synchronous and fractionally-spaced equalizers over a variety of voice-grade private-line channels.

Many years have elapsed between Lucky's invention of the adaptive synchronous equalizer,[9] Gersho's[3] and Brady's[4,10] early work on FSEs, and our present interest in fractionally-spaced equalization. This is due to both the increased complexity required to implement the FSE, and the relatively satisfactory performance of the conventional synchronous equalizer. Recent investigators have regarded the FSE primarily as a means for mitigating the timing jitter produced by an envelope-derived timing recovery system.[5,11] Our viewpoint, however, is that this property is just an example of the salient feature of the FSE—the ability to effectively compensate for an extremely wide range of delay distortion, and to deal more effectively with amplitude distortion than the synchronous equalizer.

In Section II we describe why an FSE has the ability to compensate for an arbitrary receiver sampling phase. Performance, as measured by the equalized mean-squared error, of an infinitely-long passband FSE is derived in Section III, and the corresponding results for a finite-length equalizer are described in Section IV. Simulation results, for typical voice-grade channels, are presented in Section V, and these results are used to compare the performance of the synchronous equalizer, the FSE, and the FSE with a decision-feedback section.

II. BASEBAND DESCRIPTION OF FRACTIONALLY-SPACED EQUALIZERS

We begin with a brief discussion of the ability of an FSE to compensate for any receiver timing phase. To do this we need the transfer function of a baseband fractionally-spaced equalizer. Consider the received signal

$$r(t) = \sum_m a_m f(t - mT) + \nu(t), \qquad (1)$$

where $\{a_n\}$ is the discrete multilevel data sequence, $1/T$ is the symbol rate, $f(t)$ is the system pulse response, and $\nu(t)$ is additive noise. As shown in Fig. 1, we denote excess bandwidth of the pulse $f(t)$ by α. The input to a *conventional synchronous* digital equalizer are samples of the filtered received signal at the instants $t = nT + \hat{\tau}$, i.e.,

$$r(n\dot{T} + \hat{\tau}) = r_n(\hat{\tau}) = \sum_m a_m f(nT - mT + \hat{\tau}) + \nu(nT + \hat{\tau}). \qquad (2)$$

The noiseless output of this nonrecursive digital filter, with tap weights $\{c_l\}$, is the sample sequence

$$u(nT + \hat{\tau}) = \sum_m a_m h(nT - mT + \hat{\tau}), \qquad (3)$$

where the equalized pulse samples, $h(nT)$, have a (Nyquist-equivalent) Fourier transform

$$H_T(\omega) = \sum_l c_l e^{-j\omega lT} \sum_k F\left(\omega + k\frac{2\pi}{T}\right) \exp\left[j\left(\omega + k\frac{2\pi}{T}\right)\hat{\tau}\right]$$

$$= C_T(\omega) F_T(\omega). \qquad (4)$$

Here, $F_T(\omega)$ is the aliased spectrum of $F(\omega)$, $C_T(\omega)$ is the (periodic) transfer function of the equalizer, and, ideally, the equalizer output is the data symbol, i.e., $u(nT + \hat{\tau}) = a_n$.

Recall[8] that the Nyquist-equivalent or folded (aliased) spectrum is the relevant transform when dealing with sampled-data systems. In particular, since $C_T(\omega) = C_T(\omega + k2\pi/T)$, the synchronously-spaced equalizer can only act to modify $F_T(\omega)$, as opposed to directly modifying $F(\omega)^{j\omega\hat{\tau}}$. In other words, the synchronous equalizer cannot exercise independent control over both sides of the rolloff region about $\omega =$
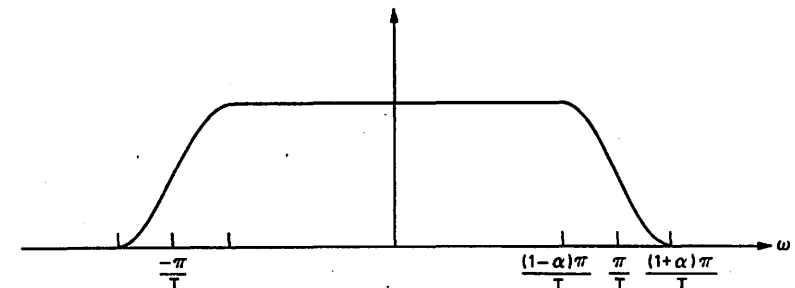

Fig. 1—Fourier transform $F(\omega)$ of baseband pulse $f(t)$ in eq. (1).
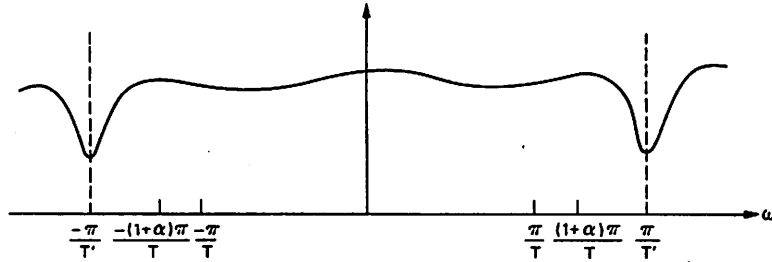
Fig. 2—Representative transfer function of a fractionally-spaced equalizer [tap spacing = T' $T/(1 + \alpha)$].

π/T. If, because of a severe phase characteristic and a poor choice of $\hat{\tau}$, a null is created in the rolloff portion* of the folded spectrum $F_T(\omega)$, then all the conventional equalizer can do to compensate for this null is to synthesize a rather large gain in the affected region; this leads to a severe performance degradation because of the noise enhancement at these frequencies.

Consider, on the other hand, a receiver which uses a *fractionally-spaced* equalizer with taps spaced $T' < T/(1 + \alpha)$ seconds apart. This equalizer has the (periodic) transfer function:

$$C_{T'}(\omega) = \sum_l c_l e^{-j\omega l T'}. \tag{5}$$

Note that if $\pi/T' \geq (1 + \alpha)\pi/T$, then the first repetition interval of the transfer function $C_{T'}(\omega)$ includes the rolloff portion of the spectrum, as shown in Fig. 2. We assume that, for digital implementation purposes, T' is generally an appropriate rational fraction of T. For an FSE receiver the equalizer input is sampled at the rate T', but the equalizer output is still sampled at the rate T, since data decisions are made at symbol intervals. The equalized spectrum, just *prior* to the output sampler, is periodic (with period $2\pi/T'$) and is given by

$$H_{T'}(\omega) = C_{T'}(\omega) \sum_k F\left(\omega + k\frac{2\pi}{T'}\right) \exp\left[j\left(\omega + k\frac{2\pi}{T'}\right)\hat{\tau}\right], \tag{6}$$

and for systems where $\pi/T' \geq (1 + \alpha)\pi/T$ only the $k = 0$ term survives, i.e.,

$$H_{T'}(\omega) = C_{T'}(\omega)F(\omega)e^{j\omega\hat{\tau}}, \qquad |\omega| \leq \frac{\pi}{T'}. \tag{7}$$

The salient aspect of (7) is that $C_{T'}(\omega)$ acts on $F(\omega)e^{j\omega\hat{\tau}}$ *before* aliasing, with respect to the output sampling rate, is performed. Thus $C_{T'}(\omega)$ can compensate for any timing phase—or phase distortion—by syn-

thesizing a transfer characteristic of the form $e^{j\omega\hat{\tau}}$. Clearly, such compensation is highly desirable since it minimizes noise enhancement and avoids the extreme sensitivity to timing phase associated with the conventional equalizer.* After sampling the equalizer output at the rate $1/T$, the output spectrum is periodic with period $2\pi/T$ and is given by

$$H_T(\omega) = \sum_l H_{T'}\left(\omega + l\frac{2\pi}{T}\right)$$

$$= \sum_l C_{T'}\left(\omega + l\frac{2\pi}{T}\right)F\left(\omega + l\frac{2\pi}{T}\right)\exp\left[-j\left(\omega + l\frac{2\pi}{T}\right)\hat{\tau}\right]. \tag{8}$$

Note that (8) differs from (4) in that it is the sum of equalized aliased components rather than an equalization of an already-formed sum of aliased components.

It is evident that an FSE is capable of much more than compensating for a poor choice of timing phase. With a properly chosen tap spacing ($T' \leq [1/(1 + \alpha)]T$), the FSE has the capabilities of an analog filter. Hence the FSE can be configured as the best linear receiver. In Section III we derive the structure and performance of such a receiver for a passband modem.

III. PERFORMANCE AND STRUCTURE OF THE OPTIMUM FSE

3.1 QAM systems

The receiver minimizing the mean-squared error is known to consist of a matched filter followed by a synchronous sampler.[8] Our discussion in Section II demonstrated the equivalence of an appropriately sampled fractionally-spaced equalizer with an analog receiver. We begin by writing the transmitted signal $s(t)$, in an in-phase and quadrature, or quadrature amplitude modulated (QAM), data transmission system as the *real* part of the analytical signal

$$\tilde{s}(t) = s(t) + j\check{s}(t) = \sum_n \tilde{d}_n p(t - nT)e^{j\omega_c t}, \tag{9}$$

where $\tilde{d}_n$ denotes the complex† discrete-multilevel data sequence, $a_n + jb_n$, $p(t)$ is the (generally real) baseband transmitter pulse shaping, $1/T$ is the symbol rate, ω_c is the radian carrier frequency, and $\check{s}(t)$ is the Hilbert transform of $s(t)$. In our presentation we will make extensive use of complex notation to denote either passband or in-phase and quadrature signals, as well as system pulse responses. A discussion

---

* This is the frequency range $(1 - \alpha)\pi/T \leq \omega \leq (1 + \alpha)\pi/T$.

* In the synchronous equalizer, a "bad" timing phase is one which produces nulls in the folded spectrum of $F_T(\omega)$ of (4). In the FSE, a "good" timing phase is generated, regardless of the input sampling epoch, such that the FSE does a minimum of amplitude enhancement.

† The overtilde, ~, is used to denote complex signals and samples.

of this approach is presented in the appendix. As shown in Fig. 3, $s(t)$ is transmitted through the passband (around ω_c) channel $x(t)$, with impulse response

$$x(t) = x_1(t) \cos\omega_c t - x_2(t) \sin\omega_c t$$
$$= \text{Re}\{(x_1(t) + jx_2(t))e^{j\omega_c t}\} = \text{Re}\{\tilde{x}_B(t)e^{j\omega_c t}\}, \qquad (10)$$

where the complex baseband-equivalent channel is defined by

$$\tilde{x}_B(t) = x_1(t) + jx_2(t). \qquad (11)$$

Thus the received analytic signal has the representation

$$\bar{r}(t) = r(t) + j\check{r}(t) = \sum_n \bar{d}_n \bar{f}_B(t - nT)e^{j(\omega_c t + \theta)} + \bar{v}(t)e^{j\omega_c t}, \qquad (12)$$

where $r(t)$ and $\check{r}(t)$ are the in-phase and quadrature components of the received signal (and are a Hilbert transform pair), $\bar{f}_B(t)$ is the baseband-equivalent received pulse which is given by the convolution of $\tilde{x}_B(t)$ with $p(t)$, θ is the channel phase shift, and $\bar{v}(t)$ is the complex noise signal.

At this point we may consider either a passband equalizer, which operates directly on $\bar{r}(t)$, or a baseband receiver which processes $\bar{r}(t) \exp[-j(\omega_c t + \theta)]$—assuming that carrier-phase coherence[2] has been established. From a mathematical viewpoint both systems are equivalent, and here we find it convenient to filter the demodulated signal,

$$\bar{q}(t) = \bar{r}(t)e^{-j(\omega_c t + \theta)} = \sum_n \bar{d}_n \bar{f}_B(t - nT), \qquad (13)$$
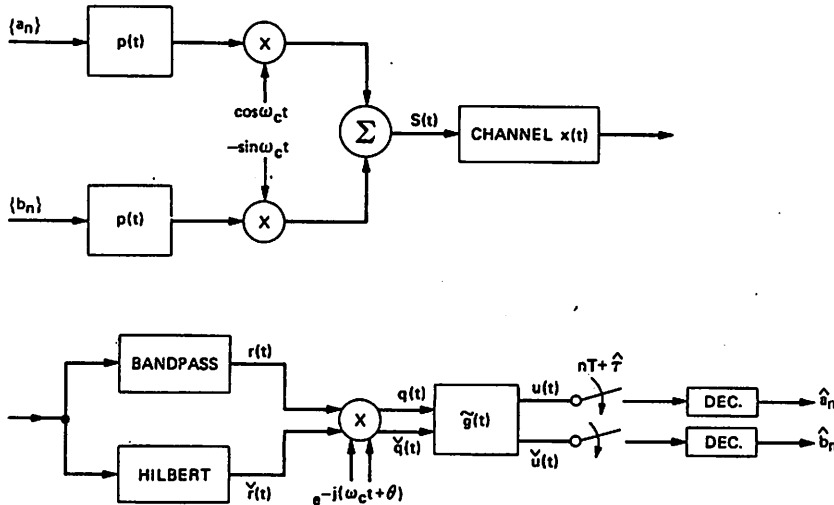

Fig. 3—QAM data transmission system. Variables with overtildes are complex, i.e., they have in-phase and quadrature components.

by the receiving filter

$$\bar{g}(t) = g_1(t) + jg_2(t). \qquad (14)$$

In writing (14) we have used the notation $g_1(t)$ and $g_2(t)$ rather than $g(t)$ and $\check{g}(t)$ to emphasize that the receiving filter does *not* correspond to an analytic pulse. Note, however, that the equalized signal at the filter output is given by the analytic signal

$$\bar{u}(t) = \bar{q}(t) \circledast \bar{g}(t) = (q(t) + j\check{q}(t)) \circledast (g_1(t) + jg_2(t))$$
$$= (q(t) \circledast g_1(t) - \check{q}(t) \circledast g_2(t))$$
$$\quad + j(\check{q}(t) \circledast g_1(t) + q(t) \circledast g_2(t))$$
$$= u(t) + j\check{u}(t), \qquad (15)$$

i.e., $u(t)$ and $\check{u}(t)$ are a Hilbert transform pair. As shown in Fig. 3 the in-phase and quadrature output signals $u(t)$ and $\check{u}(t)$ are synchronously sampled at $t = nT + \hat{\tau}$ and quantized to provide the data decisions $\hat{a}_n$ and $\hat{b}_n$.

3.2 The mean-squared error

Our attention now turns to finding the linear filter, $\bar{g}(t)$, which minimizes the output mean-squared error. The output or equalized, mean-squared error (MSE), which is the performance measure commonly used for in-phase and quadrature data transmission systems, is given as

$$\mathscr{E} = E(|\bar{e}_n|^2) = E\{e_n^2 + \check{e}_n^2\}$$
$$= E\{(u(nT) - a_n)^2 + (\check{u}(nT) - b_n)^2\}$$
$$= E(|\bar{u}(nT) - \bar{d}_n|^2), \qquad (16)$$

where E denotes the ensemble average with respect to the data symbols and the additive noise, $\bar{e}_n$ is the complex error sample, and e_n and $\check{e}_n$ are the in-phase and quadrature errors, respectively. For convenience, we have absorbed the receiver's sampling phase, $\hat{\tau}$, into the pre-equalizer pulse response by incorporating the transfer function $e^{j\omega \hat{\tau}}$ into the transform of $\bar{f}_B(t)$. In terms of the equalized pulse, $\bar{h}(t)$, defined by

$$\bar{h}(t) = \bar{f}_B(t) \circledast \bar{g}(t), \qquad (17)$$

the filter output is

$$\bar{u}(t) = \sum_n \bar{d}_n \bar{h}(t - nT) + \bar{v}(t), \qquad (18)$$

where the filtered noise, $\bar{v}(t)$, is defined by

$$\bar{v}(t) = \bar{v}(t) \circledast \bar{g}(t). \qquad (19)$$

With these definitions in mind we can write the MSE as

$$\mathscr{E} = E\{(\tilde{u}(nT) - \tilde{d}_n)(\tilde{u}(nT) - \tilde{d}_n)^*\}$$

$$= E\{\tilde{u}(nT)\tilde{u}^*(nT) - \tilde{d}_n\tilde{u}^*(nT) - \tilde{d}_n^*\tilde{u}(nT) + \tilde{d}_n\tilde{d}_n^*\}. \quad (20)$$

Using the independence of the data symbols and the independence of the noise samples, $\tilde{v}(nT)$, the terms in (20) are readily evaluated. The first term is the quadratic form

$$E\{\tilde{u}(nT)\tilde{u}^*(nT)\} = E[|\tilde{d}_n|^2] \sum_m |\tilde{h}(mT)|^2 + E[\tilde{v}(nT)\tilde{v}^*(nT)]$$

$$= E[|\tilde{d}_n|^2] \int\int [\tilde{A}(t,\tau)$$

$$+ \sigma^2\delta(t-\tau)]\tilde{g}^*(t)\tilde{g}(\tau)\, dt\, d\tau, \quad (21)$$

where $\sigma^2 = E[|\tilde{v}(nT)|^2]/E[|\tilde{d}_n|^2]$, and the Hermitian kernel, $\tilde{A}(t,\tau)$, is given by

$$\tilde{A}(t,\tau) = \sum_n \tilde{f}_B(nT - t)\tilde{f}_B^*(nT - \tau). \quad (22)$$

Note that (21) can be written compactly as the quadratic form $(\tilde{g}^*, \mathscr{A}\tilde{g})$, where $\tilde{g}$ corresponds to $\tilde{g}(t)$, $\mathscr{A}$ is the Hermitian integral operator with kernel $\tilde{A}(t,\tau) + \sigma^2\delta(t-\tau)$, and $(\mathbf{x}, \mathbf{y})$ denotes the inner product $\int x(t)y(t)\, dt$. By straightforward evaluations, the second and third terms in (20) are seen to be

$$E(\tilde{d}_n\tilde{u}^*(nT)) = E[|\tilde{d}_n|^2] \int \tilde{f}_B^*(-t)\tilde{g}^*(t)\, dt,$$

$$E(\tilde{d}_n^*u(nT)) = E[|\tilde{d}_n|^2] \int \tilde{f}_B(-t)\tilde{g}(t)\, dt. \quad (23)$$

Combining (20) to (23) the MSE, normalized by $E[|\tilde{d}_n|^2]$, has the compact representation

$$\mathscr{E} = (\tilde{g}^*, \mathscr{A}\tilde{g}) - (\tilde{f}_B^*, \tilde{g}^*) - (\tilde{f}_B, \tilde{g}) + 1, \quad (24)$$

which is a quadratic form, where $\mathscr{A}$ is recognized as being a Hermitian operator (its kernel is conjugate symmetric).

3.3 The optimum filter

The MSE, given by (24), is minimized by taking the gradient with respect to $\tilde{g}$. The optimum filter is given as the solution of the integral equation,

$$\int [\tilde{A}(t,\tau) + \sigma^2\delta(t-\tau)]\tilde{g}(\tau)\, d\tau = \tilde{f}_B(-t), \quad (25a)$$

or the equivalent operator equation

$$\mathscr{A}\tilde{g} = \tilde{f}_B. \quad (25b)$$

It turns out that the solution

$$\tilde{g}_{opt} = \mathscr{A}^{-1}\tilde{f}_B \quad (26)$$

can be explicitly determined. This is accomplished by writing the left-hand side of (25) as

$$\int \left(\sum_n \tilde{f}_B(nT - t)\tilde{f}_B^*(nT - \tau) + \sigma^2\delta(t-\tau)\right)\tilde{g}(\tau)\, d\tau$$

$$= \sum_n \tilde{f}_B(nT - t) \int \tilde{f}_B^*(nT - \tau)\tilde{g}(t)\, d\tau + \sigma^2\tilde{g}(t)$$

$$= \sum_n \tilde{z}_n\tilde{f}_B(nT - t) + \sigma^2\tilde{g}(t), \quad (27)$$

where $\tilde{z}_n = \int \tilde{f}_B^*(nT - \tau)\tilde{g}(\tau)d\tau$ are the equalized pulse samples. Equating (27) to the right-hand side of (25) gives

$$\sum_n \tilde{z}_n\tilde{f}_B(nT - t) + \sigma^2\tilde{g}(t) = \tilde{f}_B(-t), \quad (28)$$

which indicates that the optimum filter has the representation

$$\tilde{g}_{opt}(t) = \sum_n \tilde{c}_n\tilde{f}_B(nT - t), \quad (29)$$

where the $\tilde{c}_n$'s are to be determined. The solutions as represented by (29), is recognized as the cascade[8] of a synchronously-sampled filter matched to $\tilde{f}_B(t)$, and a synchronously-spaced tapped delay line with weights $\{\tilde{c}_n\}$. To solve for the $\{\tilde{c}_n\}$ we substitute (29) into (25), giving

$$\int \sum_n \tilde{f}_B(nT - t)\tilde{f}_B^*(nT - \tau) \sum_m \tilde{c}_m\tilde{f}_B(mT - t)\, d\tau$$

$$+ \sigma^2 \sum_n \tilde{c}_n\tilde{f}_B(nT - t) = \tilde{f}_B(-t), \quad (30)$$

and if we define the channel-correlation function,

$$\tilde{f}_{m-n} = \int \tilde{f}_B^*(nT - \tau)\tilde{f}_B(mT - \tau)\, d\tau, \quad (31)$$

then we can rewrite (30) as

$$\sum_n \sum_m \tilde{f}_{n-m}\tilde{c}_m\tilde{f}_B(nT - t) + \sigma^2 \sum_n \tilde{c}_n\tilde{f}_B(nT - t) = \tilde{f}_B(-t). \quad (32)$$

Taking Fourier transforms on both sides of (32), with respect to the

continuous variable t, gives

$$\sum_n \sum_m \tilde{h}_{n-m} \tilde{c}_m \bar{F}_B^*(\omega) e^{j\omega nT} + \sigma^2 \sum_n \tilde{c}_n e^{j\omega nT} \bar{F}_B^*(\omega) = \bar{F}_B^*(\omega), \qquad (33)$$

where $\bar{F}_B(\omega)$ is the transform of $\tilde{f}_B(t)$. Dividing through by $\bar{F}_B^*(\omega)$, over the region where the channel does not vanish, we can rewrite (33) as

$$\tilde{\mathscr{F}}(\omega) \tilde{C}_T(\omega) + \sigma^2 \tilde{C}_T(\omega) = 1, \qquad (34)$$

where the following Fourier transforms, with respect to the discrete-time variables, are identified by

$$\tilde{C}_T(\omega) = \sum_n \tilde{c}_n e^{j\omega nT},$$

$$\tilde{\mathscr{F}}(\omega) = \sum_n \tilde{h}_n e^{j\omega nT} = \frac{1}{T} \sum_l \left| \bar{F}_B\left(\omega + l\frac{2\pi}{T}\right) \right|^2. \qquad (35)$$

The transform $\tilde{\mathscr{F}}(\omega)$ corresponds to the synchronously-sampled matched filter pulse, $\tilde{f}_B(t) \circledast \tilde{f}_B^*(t)$, and $\tilde{C}_T(\omega)$ is the transform of the coefficients of the synchronously-spaced tapped delay line. From (34) we have that

$$\tilde{C}_T(\omega) = \frac{1}{\tilde{\mathscr{F}}(\omega) + \sigma^2} = \frac{1}{(1/T) \sum_l |\bar{F}_B(\omega + l2\pi/T)|^2 + \sigma^2}, \qquad (36)$$

and thus the optimum linear receiver has the transform

$$\tilde{G}_{\text{opt}}(\omega) = \tilde{C}_T(\omega) \bar{F}_B^*(\omega) = \frac{\bar{F}_B^*(\omega)}{(1/T) \sum_l |\bar{F}_B(\omega + l2\pi/T)|^2 + \sigma^2}. \qquad (37)$$

The final transform of interest is that of the equalized baseband-equivalent pulse, which is

$$\tilde{H}(\omega) = \frac{|\bar{F}_B(\omega)|^2}{(1/T) \sum_l |\bar{F}_B(\omega + l\,2\pi/T)|^2 + \sigma^2}. \qquad (38)$$

Since $\tilde{H}(\omega)$ is real, the real part $h_1(t)$ and imaginary part $h_2(t)$ of its inverse Fourier transform are even and odd functions of time, respectively. Moreover, as $\sigma^2 \to 0$ it is also clear that $H_{\text{eq}}(\omega) = (1/T) \sum_k \tilde{H}(\omega + k\,2\pi/T) = 1$, i.e., not surprisingly, the equalized channel is Nyquist. From (24) to (26) it follows that the minimized MSE is

$$\mathscr{E}_{\text{opt}} = 1 - (\tilde{\mathbf{f}}_B, \mathscr{A}^{-1}\tilde{\mathbf{f}}_B) = 1 - (\tilde{\mathbf{f}}_B, \tilde{\mathbf{g}})$$

$$= 1 - \int_{-\infty}^{\infty} \bar{F}_B(\omega) \tilde{G}_{\text{opt}}(\omega) \frac{d\omega}{2\pi}, \qquad (39)$$

which can be rewritten as

$$\mathscr{E}_{\text{opt}} = 1 - \int_{\pi/T}^{\pi/T} \frac{\sum_k |\bar{F}_B(\omega + k\,2\pi/T)|^2}{(1/T) \sum_l |\bar{F}_B(\omega + l\,2\pi/T)|^2 + \sigma^2} \frac{d\omega}{2\pi}. \qquad (40)$$

In summary, eqs. (37) to (40) give a complete description of the performance and structure of the optimum linear receiver. The structure is equivalent to an infinitely-long fractionally-spaced equalizer whose taps are spaced close enough to accommodate the bandwidth of the transmitted signal. Finally note that, as expected, the phase characteristics of the channel, including the timing phase, do not enter into the expression for the minimum MSE; thus, the steady-state system performance is independent of these characteristics.

IV. THE FINITE-LENGTH FRACTIONALLY SPACED EQUALIZER

In this section we first describe the steady-state performance of finite-length FSEs, and then demonstrate that, even as the noise vanishes, such an equalizer always has a unique tap setting.

4.1 Steady-state performance

Here we consider the mean-squared error of a finite-length fractionally spaced equalizer. The demodulated received signal,[*] (13), is sampled at the rate $1/T'$, and thus the equalizer input is

$$q(nT') = \sum_m \tilde{d}_m \tilde{f}_B(nT' - mT) + v(nT'). \qquad (41)$$

We make a slight change in notation by letting $\tilde{c}_n$ denote the complex equalizer taps—thus the transfer function $\tilde{G}(\omega)$ of the previous section is replaced by $\tilde{C}(\omega)$. The equalizer output, which is only needed at the synchronous instants, is given by

$$\tilde{u}(nT) = \sum_{m=-N}^{N} \tilde{c}_m \tilde{q}(nT - mT'), \qquad (42)$$

where the equalizer has $2N + 1$ complex taps. For the finite-length equalizer the MSE is written compactly as

$$\mathscr{E} = E(e_n^2 + \tilde{e}_n^2) = E(|\tilde{u}(nT) - \tilde{d}_n|^2)$$

$$= E\{|\tilde{\mathbf{c}}' \tilde{\mathbf{q}}_n - \tilde{d}_n|^2\}, \qquad (43)$$

---

[*] A passband equalizer, in which the demodulator follows the equalizer, has the same performance against linear distortion as does the baseband equalizer. The passband and baseband equalizer differ in their performance in the presence of phase jitter.

where the tap vector and the delay-line sample vector are given by

$$\tilde{c}' = (\tilde{c}_{-N}, \cdots, \tilde{c}_N),$$

$$\tilde{q}'_n = (\tilde{q}(nT + NT'), \cdots, \tilde{q}(nT), \cdots, \tilde{q}(nT - NT')), \qquad (44)$$

and the vectors with an asterisk will denote the transposed conjugate vector. Performing the indicated expectation gives

$$\mathscr{E} = \tilde{c}^* \bar{A} \tilde{c} - (\tilde{c}^* f_B + \tilde{f}_B^* \tilde{c}) + \sigma_d^2, \qquad (45)\dagger$$

where the $(2N + 1) \times (2N + 1)$ Hermitian channel-correlation matrix, the $(2N + 1) \times 1$ channel vector, and the data power are defined, respectively, by

$$\bar{A} = E(\tilde{q}_n \tilde{q}_n^*),$$

$$\tilde{f}_B = E(\tilde{d}_n^* \tilde{q}_n), \qquad ,$$

$$\sigma_d^2 = E(|\tilde{d}_n|^2). \qquad (46)$$

It is interesting to compute the klth element, $\bar{A}_{kl}$, of the channel-correlation matrix; a direct calculation gives

$$\bar{A}_{kl} = E(\tilde{q}(nT - kT')\tilde{q}^*(nT - lT'))$$

$$= \sigma_d^2 \sum_m \tilde{f}_B(mT - kT')\tilde{f}_B^*(mT - lT') + \sigma^2 \delta_{k-l}, \qquad (47)$$

where δ_{k-l} is the Kronecker delta. Note that in contrast to the synchronous equalizer, the channel-correlation matrix is Hermitian but *not* Toeplitz. To explicitly see the non-Toeplitz nature of the $\bar{A}$ matrix we can rewrite (47) in the frequency domain as

$$\frac{1}{\sigma_d^2}(\bar{A}_{k-l} - \sigma^2 \delta_{k-l})$$

$$= \int_{-\pi/T}^{\pi/T} \left\{ \sum_m \tilde{F}_B\left(\omega + m\frac{2\pi}{T}\right) \exp\left[-j\left(\omega + m\frac{2\pi}{T}\right)kT'\right] \right\}$$

$$\cdot \left\{ \sum_n \tilde{F}_B^*\left(\omega + n\frac{2\pi}{T}\right) \exp\left[j\left(\omega + n\frac{2\pi}{T}\right)lT'\right] \right\} \frac{d\omega}{2\pi}$$

$$= \int_{-\pi/T}^{\pi/T} e^{-j\omega(k-l)T'}\left[\sum_m \tilde{F}_B\left(\omega + m\frac{2\pi}{T}\right)e^{-jmk2\pi T'/T}\right]$$

$$\cdot \left[\sum_n \tilde{F}_B^*\left(\omega + n\frac{2\pi}{T}\right)e^{jnl2\pi T'/T}\right] \frac{d\omega}{2\pi}, \qquad (48)$$

and for systems with nonzero excess bandwidth the bracketed terms depend on k and l individually, rather than on $k - l$. Recall that for the synchronous equalizer $T' = T$ and A_{kl} depends only on $k - l$.

For completeness note that the channel vector $\tilde{f}_B$ has the lth element

$$(\tilde{f}_B)_l = E(\tilde{d}_n \tilde{q}(nT - lT')) = E(|\tilde{d}_n|^2)\tilde{f}_B(lT'). \qquad (49)$$

In terms of the above parameters, it is evident from (45) that the optimum tap setting is†

$$\tilde{c}_{\text{opt}} = \bar{A}^{-1}\tilde{f}_B \qquad (50)$$

and the minimized MSE is

$$\mathscr{E}_{\text{opt}} = 1 - \tilde{f}_B^* \bar{A}^{-1}\tilde{f}_B. \qquad (51)$$

4.2 The adaptive algorithm

As with the conventional passband equalizer,[1-2] the adaptive control algorithm makes use of the gradient of the sum of the squared in-phase error and the squared quadrature error with respect to the tap weights. Taking these derivatives, and writing the result in complex notation gives the adjustment algorithm

$$\tilde{c}_{n+1} = \tilde{c}_n - \alpha \tilde{e}_n \tilde{q}_n^*, \qquad n = 0, 1, 2, \cdots, \qquad (52)$$

where $\tilde{c}_n$ is the complex tap vector at the nth iteration, and α is a positive number, called the step size, which affects the algorithm's rate of convergence and the fluctuation about the minimum-attainable steady-state MSE. Note that the algorithm is updated once per symbol interval, but it is conceivable that adjustments could be made more frequently if the mid-symbol output levels can be interpolated reasonably well. Reference 12 gives a detailed analytic and experimental treatment of the convergence rate and some of the dynamic aspects of FSES.

4.3 Does a finite-length fractionally-spaced equalizer have a unique tap setting?

To answer the question posed by the title of this section we return to the baseband data transmission system discussed in Section II. The transmitted spectrum, as shown in Fig. 1, is bandlimited to $(1 + \alpha) \pi/ T$ rad/s, where the rolloff factor, α, varies from 0 to 1. From Fig. 2 it should also be evident that when the noise becomes vanishingly small, there is legitimate concern as to what function(s) the equalizer will

---

† Recall that for any two complex vectors $\tilde{x}$ and $\tilde{v}$, $\tilde{x}^* \tilde{v} = (\tilde{v}^* \tilde{x})^*$.

† A little care must be exercised in differentiating the MSE with respect to $\tilde{c}$, since $\tilde{c}^*\tilde{c}$ is *not* an analytic function of $\tilde{c}$. The most compact approach is to differentiate the MSE, with respect to the real and imaginary components of $\tilde{c}$, and to then interpret the gradient as a complex vector.

synthesize in the region $(1 + \alpha)\ \pi/T < \omega < 2\pi/T$, where there is no signal energy. In terms of the channel correlation matrix given by (47), we note that the matrix A is the sum of two matrices, and, as will be evident from the discussion which follows, the channel-dependent component of A is always positive semidefinite. Since the other component of the channel-correlation matrix, $\sigma^2 I$, is positive definite, then A will also be positive definite, and we can conclude that when there is noise present the optimum tap setting is unique.

We now consider the situation as the noise becomes vanishingly small; clearly from (50), the optimum tap setting is unique if and only if A is nonsingular. A sufficient condition for A to be nonsingular is the nonvanishing of the quadratic form $\mathbf{u}'A\mathbf{u}$, for any *nonzero* test vector $\mathbf{u}$ with components $\{u_i\}$. Let us consider in detail this quadratic form, which we write from (47) as

$$\mathbf{u}'A\mathbf{u} = \sum_{m,n=-N}^{N} u_m A_{mn} u_n$$

$$= \sum_{m,n=-N}^{N} u_m u_n \sum_{l=-\infty}^{\infty} f(lT - nT')f(lT - mT')$$

$$= \sum_{l=-\infty}^{\infty} \left[\sum_{m=-N}^{N} u_m f(lT - mT') \right]^2 \geq 0. \qquad (53)$$

The above inequality establishes the positive semidefinite nature of the matrix A, and we see from, (53) that $\mathbf{u}'A\mathbf{u}$ can vanish only if [*]

$$\sum_{m=-N}^{N} u_m f(lT - mT') = 0, \qquad l = 0, \pm 1, \pm 2, \cdots. \qquad (54)$$

If we define the periodic Fourier transform

$$U_{T'}(\omega) = \sum_{m=-N}^{N} u_m e^{j\omega m T'}, \qquad |\omega| \leq \frac{\pi}{T'}, \qquad (55)$$

then we can proceed further by noting that

$$\sum_{m=-N}^{N} u_m f(lT - mT') = \sum_{m=-N}^{N} u_m \int_{-\infty}^{\infty} F(\omega)e^{j\omega(lT - mT')} \frac{d\omega}{2\pi}$$

$$= \int_{-\infty}^{\infty} \left[\sum_{m=-N}^{N} u_m e^{-j\omega m T'} \right] F(\omega)e^{-j\omega lT} \frac{d\omega}{2\pi}$$

$$= \int_{-\infty}^{\infty} U_{T'}(\omega)F(\omega)e^{-j\omega lT} \frac{d\omega}{2\pi}$$

$$= \sum_{k} \int_{(2k-1)(\pi/T)}^{(2k+1)(\pi/T)} U_{T'}(\omega)F(\omega)e^{-j\omega lT} \frac{d\omega}{2\pi}$$

$$= \int_{-\pi/T}^{\pi/T} \left[\sum_{k} U_{T'}\left(\omega + \frac{k2\pi}{T}\right)F\left(\omega + \frac{k2\pi}{T}\right) \right]$$

$$\cdot e^{-j\omega lT} \frac{d\omega}{2\pi}. \qquad (56)$$

The right-hand side of (56) is recognized as the sample, at $t = lT$, of a function whose Fourier transform $Z_{eq}(\omega)$ is contained in the brackets. Now if (56) is to be zero for every value of l, then it must be that the Fourier transform inside the integral vanishes completely, i.e.,

$$Z_{eq}(\omega) \equiv \sum_{k} U_{T'}\left(\omega + \frac{k2\pi}{T}\right)F\left(\omega + \frac{k2\pi}{T}\right) = 0, \qquad |\omega| \leq \frac{\pi}{T}. \qquad (57)$$

For less than 100 percent excess bandwidth, note that only the $k = 0$, ± 1 terms contribute to the above sum. However, in the nonrolloff region, $|\omega| \leq (1 - \alpha)\ \pi/T$, only the $k = 0$ term influences the sum. For channels which do not vanish over the entire nonrolloff region, it is clear that for $Z_{eq}(\omega)$ to vanish it is required that $U_{T'}(\omega)$ vanish at least over the entire nonrolloff region. Since $U_{T'}(\omega)$ is a finite-term Fourier series, it cannot vanish over an interval without vanishing everywhere, which in turn would again make $\mathbf{u} = 0$. Note that if the channel vanished over a portion of the nonrolloff region, then since $U_{T'}(\omega)$ is a finite-term Fourier series, its energy could not be totally concentrated in the region where there was no channel energy. Thus, the solution would still be unique. However, it is worth noting that in the extreme case of 100 percent excess bandwidth, $Z_{eq}(\omega)$ can vanish. For example, consider a constant $F(\omega)$, with $U_{T'}(\omega) = \cos(\omega T/2)$. It is apparent from (57) that $Z_{eq}(\omega) \equiv 0$. Thus for a *finite-length* FSE with an excess bandwidth of less than 100 percent, we can conclude that *even as the noise becomes vanishingly small the A matrix is nonsingular and there is a unique optimum tap setting.*

Note that for a finite-length synchronous equalizer where $T' = T$, (57) indicates that since $U_T(\omega + (k2\pi/T)) = U_T(\omega)$, we can conclude that if the folded-channel spectrum does not vanish completely then there is always a unique tap setting. Reference 12 showed that as the equalizer becomes infinitely long there is an infinitude of equalizer tap vectors which achieve the same minimum mean-squared error. Consequently, it is to be expected that a FSE equalizer with a "large" number of tap weights will have many tap vectors which produce essentially the same MSE.

V. PERFORMANCE OF FRACTIONALLY-SPACED EQUALIZERS

To illustrate the advantages of fractionally-spaced equalization over synchronous equalization, a number of computer simulation runs were made for different equalizer configurations and for channel distortions of varying severity. The system tested was the 9.6 kbit/s QAM system, shown in Fig. 3, having a symbol rate of 2400/s and an excess bandwidth of 12 percent, and the transmitted-symbol alphabet, {±1, ±3}. For each run the steady-state mean-squared error was measured after a sufficiently long period of adaptation, and the FSE was of the $T/2$ type.

Amplitude and delay-distortion characteristics are illustrated in Fig. 4 for the three linear channels which were simulated. The "Good" channel is of low distortion, and well within the limits of standard conditioning, e.g., the "Basic" conditioning[13] illustrated in Fig. 5. The "Bad-Phase" and "Bad-Slope" channels have, respectively, severe phase distortion and severe amplitude distortion, placing these channels just outside the defining boundaries of basic-conditioned channels.

Figures 6, 7, and 8 compare the performance of a 24-tap synchronous (T) equalizer and a 48-tap $T/2$ equalizer on the three test channels. Performance is examined for five timing epochs within a symbol interval, and is measured by the output signal-to-noise ratio, defined as

$$\text{SNR}_{\text{out}} = \log \frac{P_{BB}}{\text{MSE}}, \qquad (58)$$

where P_{BB} is the received baseband average signal power (a constant), and MSE is the measured output mean-squared error. The received signal is normalized so that the ratio of the signal power at the output of the receiving filters to the power of the additive noise, at the same point in the system, is 28 dB. Thus if the equalizer could "undo" the channel distortion without enhancing the noise, then the output SNR would be 28 dB. It is apparent that the performance of the fractionally-spaced equalizer is almost independent of the timing epoch, in sharp contrast to that of the synchronous equalizer. This confirms the prediction of the analysis, culminating in expression (40) for the minimum mean-squared error, which is independent of the sampling epoch. It is also significant that the performance of the fractionally-spaced equalizer on the "Bad-Phase" channel is significantly better than that achieved by the synchronous equalizer even for the best sampling phase. The capability of the FSE for phase equalization, before folding the spectrum about the Nyquist frequency, is seen to be an important advantage on channels with severe phase distortion. With the addition of a decision-feedback equalizer (DFE),[14] with feed-
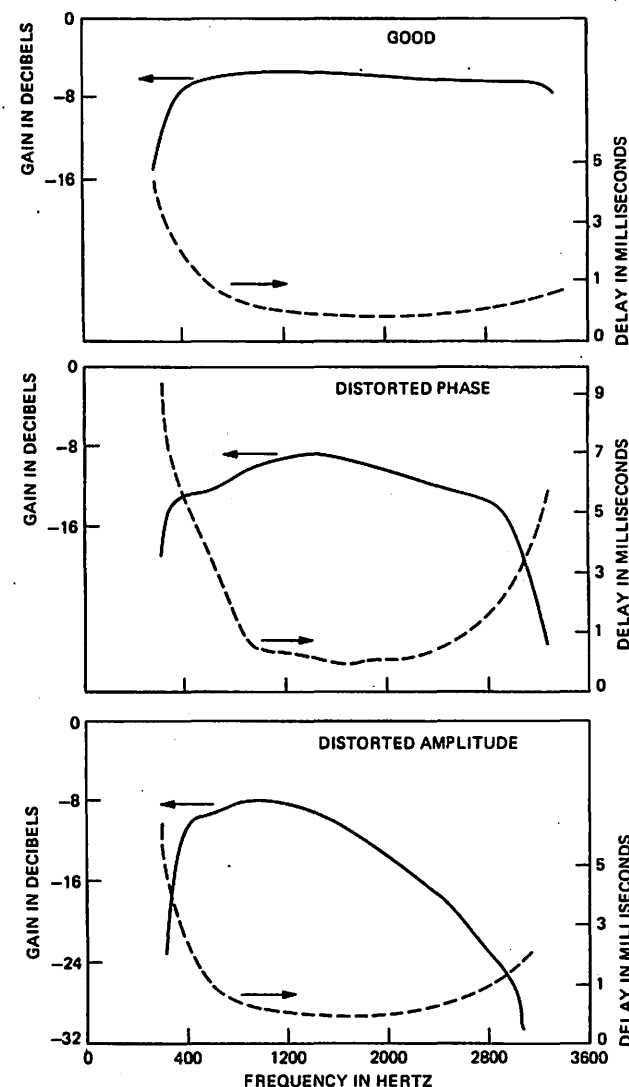

Fig. 4—Characteristics of simulated transmission channels.

back taps $\{f_i\}_{i=1}^N$, shown in Fig. 9, compensation for severe amplitude distortion is also improved, as illustrated in Fig. 8.

The simulation of an FSE with $3T/4$ tap spacing [still less than $T/(1 + \alpha)$, where $\alpha = 0.12$ was the percentage of excess bandwidth] resulted in performance comparable to that of the $T/2$ equalizer. A $3T/4$ equalizer needs only 2/3 as many taps as a $T/2$ equalizer to span
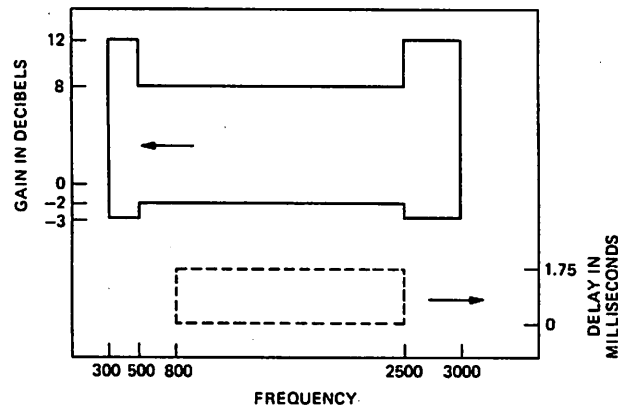
Fig. 5—Defining boundaries of "Basic"-conditioned channels.

Fig. 7—Performance on "Bad-Phase" channel of Fig. 4.

a given channel dispersion, which cannot only reduce implementation complexity, but also improve steady-state performance when digital resolution is a consideration.[12]

VI. CONCLUSIONS

We have shown, both analytically and by simulation, that the fractionally-spaced equalizer provides virtual independence from tim-
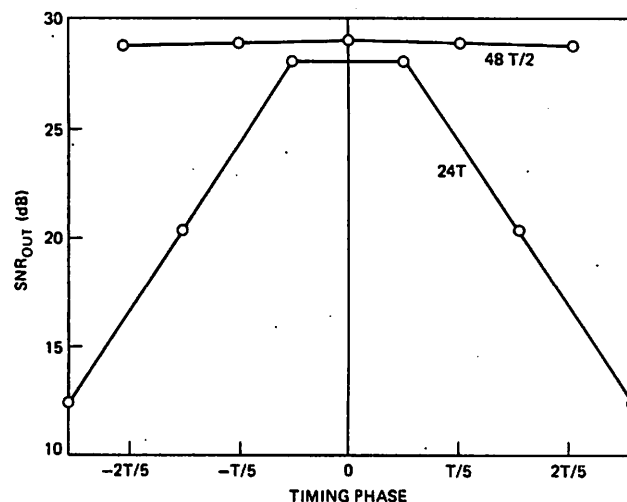
ing epoch, and significantly improves steady-state performance on severely phase-distorted channels. Implementation of the FSEs increased number of taps, with respect to a synchronous equalizer with the same total time span, is well within the capabilities of current digital signal-processing technology. The performance degradation introduced in a digital implementation by using a larger number of taps is more than compensated for by the FSEs capability of adaptively

Fig. 6—Performance versus sampling phase of 24-tap synchronous (T) equalizer and 48-tap ($T/2$) equalizer on "Good" channel of Fig. 4. Results from computer simulation of 9600 bps QAM modem.
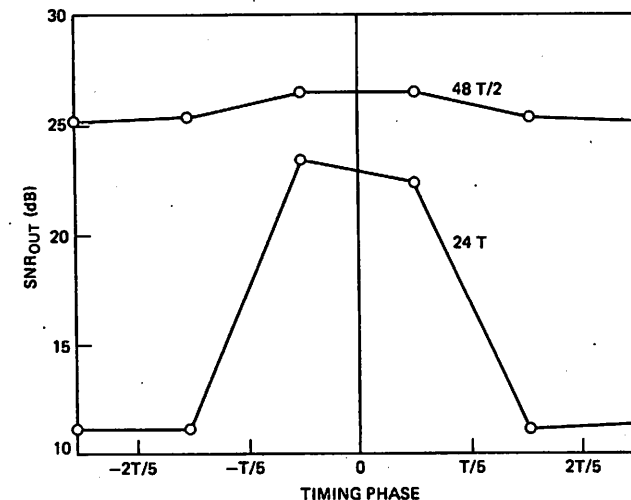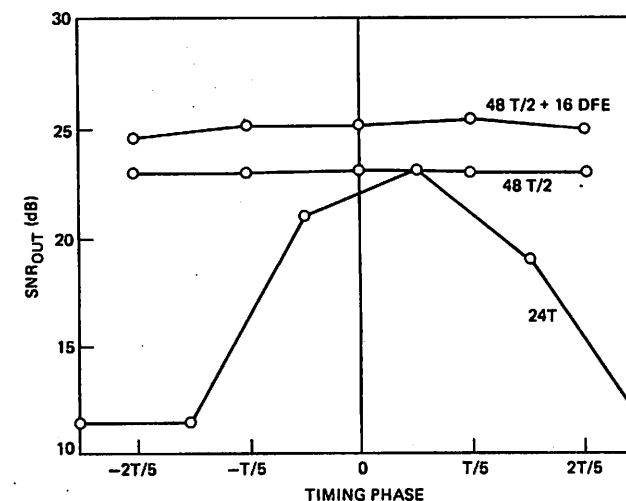

Fig. 8—Performances on "Bad-Slope" channel. The top curve is for a receiver which incorporates both a 48-tap FSE and a 16-tap decision-feedback equalizer (DFE).
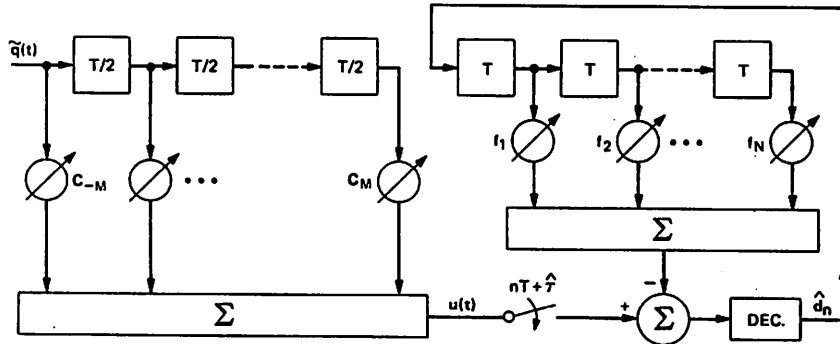
Fig. 9—QAM data receiver combining a fractionally-spaced equalizer and a decision feedback equalizer.

realizing, in one structure, the optimum receiving filter consisting of a matched filter followed by a delay line tapped at symbol intervals.

APPENDIX

Complex Notation and Passband Communication Systems

The purpose of this appendix is to review and organize the compact description provided by complex notation for the discussion of in-phase and quadrature data communications systems. In such a system the transmitted waveform is of the form

$$s(t) = \sum_n a_n p(t - nT) \cos \omega_c t - \sum_n b_n p(t - nT) \sin \omega_c t, \quad (59)$$

where $\{a_n\}$ and $\{b_n\}$ are the in-phase and quadrature data streams, $1/T$ is the symbol rate, $p(\cdot)$ is a bandlimited pulse, and ω_c is the radian carrier frequency. The signal $s(t)$ can be written as the real part of the complex analytic signal

$$\tilde{s}(t) = \sum_n \tilde{d}_n p(t - nT) e^{j\omega_c t}, \quad (60)$$

where

$$\tilde{d}_n = a_n + jb_n.$$

Recall that a signal is analytic if it only has power at positive (or negative) frequencies.[15] The analytic signal with positive frequency content is

$$\tilde{s}(t) = s(t) + j\check{s}(t), \quad (61)$$

where $\check{s}(t)$ is the Hilbert transform of $s(t)$. We now describe the output signal when $s(t)$ is transmitted through a linear passband channel that is band-limited with impulse response

$$x(t) = 2x_1(t) \cos \omega_c t - 2x_2(t) \sin \omega_c t, \quad (62)$$

where $x_1(t)$ and $x_2(t)$ are real. If we denote the Fourier transform of $x(t)$ by

$$X(\omega) = |X(\omega)| e^{j\angle X(\omega)}, \quad (63)$$

then the in-phase pulse response, $x_1(t)$, and the quadrature pulse response, $x_2(t)$, are given by

$$x_1(t) = \int_{-\omega_c}^{\infty} |X(\omega + \omega_c)| \cos[\angle X(\omega + \omega_c) + \omega t] \frac{d\omega}{2\pi},$$

$$x_2(t) = \int_{\omega_c}^{\infty} |X(\omega + \omega_c)| \sin[\angle X(\omega + \omega_c) + \omega t] \frac{d\omega}{2\pi}. \quad (64)$$

Thus, $x_1(t)$ and $x_2(t)$ are determined by the positive spectral content of the real pulse $x(t)$. In general, the baseband pulses $x_1(t)$ and $x_2(t)$ are unrelated [except through (64)], but if the transfer function $X(\omega)$ has even amplitude symmetry and odd-phase symmetry about the carrier frequency, then $x_2(t) = 0$. Also note that, in general, $x_1(t)$ and $x_2(t)$ are *not* a Hilbert transform pair.

Given the in-pulse and quadrature pulses $x_1(t)$ and $x_2(t)$, we define the analytic pulse

$$\tilde{x}(t) = 2[x_1(t) + jx_2(t)]e^{j\omega_c t} \quad (65)$$

$$= 2\tilde{x}_B(t)e^{j\omega_c t}, \quad (66)$$

where, as noted above, the complex baseband-equivalent pulse, $\tilde{x}_B(t)$ $\equiv x_1(t) + jx_2(t)$, is *not* necessarily analytic. The pulse $\tilde{x}_B(t)$ has a Fourier transform $X(\omega + \omega_c)$, $\omega > -\omega_c$; i.e., the transform is the positive frequency portion of $X(\omega)$ shifted down to the origin. The channel output signal, $s(t) \circledast x(t)$, is of course the $\text{Re}[\tilde{s}(t) \circledast \tilde{x}(t)]$, and we have that

$$\tilde{s}(t) \circledast \tilde{x}(t) = e^{j\omega_c t} \sum_n \tilde{d}_n[\tilde{p}(t - nT) \circledast \tilde{x}_B(t)], \quad (67)$$

where we have allowed the transmitted pulse, $\tilde{p}(t)$, to be "complex." By a complex transmitted pulse we mean that the pulse input is a two-dimensional vector and a cross-coupled operation defines the filter; i.e., if the filter input is the two-tuple vector $(z_1(t), z_2(t))$, which we use to define an equivalent complex signal $\tilde{z}(t) = z_1(t) + jz_2(t)$, then the output vector is $\tilde{u}(t) = \tilde{p}(t) \circledast \tilde{z}(t)$, where the outputs, $u_1(t)$ and $u_2(t)$, are the real and imaginary parts of $\tilde{u}(t)$.

At the receiver, coherent quadrature demodulation by $\cos \omega_c t$ and $\sin \omega_c t$, followed by low-pass filtering, provides the in-phase and quadrature signals; these component signals can also be derived by forming the two-tuple vector composed of the in-phase and quadrature signals (the latter signal is simply the Hilbert transform of the received signal)

and "rotating" the two tuple by $\omega_c t$ radians.[16] This latter operation corresponds to simply multiplying (67) by $\exp(-j\omega_c t)$; i.e., the demodulation signal, $\bar{r}(t)$, is given by

$$\bar{r}(t) = \sum_n \bar{d}_n \bar{f}_B(t - nT), \qquad (68)$$

where the baseband equivalent pulse $\bar{f}_B(t) \equiv \bar{p}(t) \circledast \bar{x}_B(t)$.

Thus, given the channel $x(t)$, we see that from a linear distortion viewpoint, the system is characterized by the (equivalent) baseband pulse $\bar{f}_B(t) = \bar{p}(t) \circledast \bar{x}_B(t)$. If the demodulated signal, $\bar{r}(t)$, is further filtered, or equalized, by a lattice-type filter,† $\bar{g}(t)$, the overall pulse shape will be $\bar{p}(t) \circledast \bar{x}_B(t) \circledast \bar{g}(t)$.

To summarize, we have illustrated the convenience of complex notation for representing in-phase and quadrature passband signals in terms of the equivalent baseband channel and, explicitly, the carrier frequency. Receiver operations of demodulation and lattice equalization are then easy to visualize and are compactly described as complex multiplications and convolution, respectively.

REFERENCES

1. R. D. Gitlin, E. Y. Ho, and J. E. Mazo, "Passband Equalization of Differentially Phase-Modulated Data Signals," B.S.T.J., *52*, No. 2 (February 1973), pp. 219–38.
2. D. D. Falconer, "Jointly Adaptive Equalization and Carrier Recovery in Two-Dimensional Digital Communication Systems," B.S.T.J., *55*, No. 3 (March 1976), pp. 317–34.
3. A. Gersho, private communication, 1968.
4. D. M. Brady, "An Adaptive Coherent Diversity Receiver for Data Transmission Through Dispersive Media," Conference Record, ICC 1970 (June 1970), pp. 21-35-21-40.
5. G. Ungerboeck, "Fractional Tap-Spacing Equalizers and Consequences for Clock Recovery for Data Modems," IEEE Trans. Commun., *COM-24*, No. 8 (August 1976).
6. J. E. Mazo, private communication.
7. O. Macchi and L. Guidoux, "A New Equalizer and Double Sampling Equalizer," Ann. Telecomm., *30* (1975), pp. 331–8.
8. R. W. Lucky, J. Salz, and E. J. Weldon, Jr., *Principles of Data Communication*, New York: McGraw-Hill, 1968.
9. R. W. Lucky, "Automatic Equalization for Digital Communications," B.S.T.J., *44*, No. X (April 1965), pp. 547–88.
10. D. M. Brady, Adaptive Signal Processor for Diversity Radio Receivers, U.S. Patent No. 3,633,107, January 4, 1972.
11. S. U. H. Qureshi and G. D. Forney, Jr., "Performance and Properties of a $T/2$ Equalizer," Conference Record, NTC 1977 (December 1977).
12. R. D. Gitlin and S. B. Weinstein, "On the Required Tap Weight Precision for Digitally-Implemented Adaptive Equalizers," B.S.T.J., *58*, No. 2 (February 1979), pp. 301–21.
13. Bell System Technical Reference, "Data Communications Using Voiceband Private Line Channels," PUB 41004, October 1973.
14. J. Salz, "Optimum Mean-Square Decision Feedback Equalization," B.S.T.J., *52*, No. 8 (October 1973), pp. 1431–73.
15. H. E. Rowe, *Signals and Noise in Communication Systems*, New York: Van Nostrand, 1965.
16. D. A. Spaudling, "A New Digital Coherent Demodulator," IEEE Trans. Commun., *COM-21*, No. 3 (March 1973), pp. 237–8.

---

† By a lattice filter, $\bar{g}(t) = g_1(t) + jg_2(t)$, we mean that if the in-phase and quadrature inputs are $r(t)$ and $\bar{r}(t)$, then the filter outputs are $r(t) \bullet g_1(t) - \bar{r}(t) \bullet g_2(t)$ and $\bar{r}(t) \bullet g_1(t) + r(t) \bullet g_2(t)$, respectively.